Astron. Astrophys. 334, 935–942 (1998)

ASTRONOMY AND ASTROPHYSICS

# High sensitivity search for molecular gas in the $\beta$ Pic disk$^\star$

## On the low gas-to-dust mass ratio of the circumstellar disk around $\beta$ Pictoris

**René Liseau and Pawel Artymowicz**

Stockholm Observatory, S-133 36 Saltsjöbaden, Sweden
(e-mail: rene@astro.su.se; web: http://www.astro.su.se/~rene/; e-mail: pawel@astro.su.se; web: http://www.astro.su.se/~pawel/)

Received 6 October 1997 / Accepted 4 March 1998

**Abstract.** We report on high sensitivity observations of the $\beta$ Pic system in four molecular transitions with the 15 m SEST, tracing carbon, silicon and sulphur bearing species (CO, SiO and CS) and, as such, the gaseous component of the circumstellar disk. The lack of signal in the CO (2–1) line is consistent with an interstellar value of CO/H and a very low column density of hydrogen gas [$N(\mathrm{H}) < 10^{19}\,\mathrm{cm}^{-2}$]. The data do not require that CO is severely depleted with respect to hydrogen. Rather, we find that the gas-to-dust mass ratio in the disk is abnormally low, viz. $m_{\rm gas}/m_{\rm dust} < 0.1$ ($< 0.05$ at the $1\,\sigma$ level), implying an upper limit to the mass of hydrogen gas $m(\mathrm{H}) < 2\,10^{-2}\,\mathrm{M}_\oplus$ ($5\,\mathrm{M}_{\rm Moon}$). Evidently, any nebular disk gas from the formation stage of $\beta$ Pic has been consumed in planet formation and/or blown out during the early mass loss history of the system. The sensitive search for SiO gas, believed to be presently produced in evaporative grain-grain collisions, gave likewise negative results. From the modeling of the line emission from the $\beta$ Pic disk we deduce that this non-detection could be explained by insufficient filling of the SEST beam and that the testing of the theory has to await the advent of the new generation of millimeter interferometers in the southern hemisphere.

**Key words:** stars: individual: $\beta$ Pictoris – stars: formation – stars: evolution – stars: circumstellar matter – stars: planetary systems – radio lines: stars

### 1. Introduction

The dusty circumstellar disk around the nearby (19.3 pc, Crifo et al. 1997) A5 V star $\beta$ Pic (HD 39060, HR 2020) is a uniquely prominent example of the Vega-type stars, which are characterized by infrared excess emission and which may represent a post-formation stage of planetesimal or planetary systems (for the observed high frequency of the Vega-phenomenon see, e.g., Habing et al. 1996). Our present knowledge of the $\beta$ Pic system has been summarized by, e.g., Backman & Paresce (1993), Lagrange (1995) and Artymowicz (1997). The system is well observed over nearly the entire electromagnetic spectrum, from far ultraviolet (UV) to millimeter (mm) wavelengths. As yet, no spectral features have been detected that are sharp enough to directly provide proof that the elongated dust structure of size $\gtrsim 1'$ (e.g. Kalas & Jewitt 1995) seen at the star is indeed, as is widely believed, an edge-on disk of grains in Keplerian rotation around the central star. As a first step, before actually attempting to map the rotation curve, one needs to identify and detect appropriate spectral tracers of the velocity field. Rotational transitions in molecules, thought to accompany the relatively cool grains, seem a natural option.

In the outer parts of the disk ($r > 30$ AU), considerable amounts of $H_2O$ and CO molecules from sublimated/sputtered icy grains could be expected. In addition, comets may release CO both far (many AU) from the star and in its vicinity (Beust et al. 1994). From UV absorption lines toward the star a column density of $(2.0 \pm 0.5)\,10^{15}\,\mathrm{cm}^{-2}$ of CO gas at a temperature of 20 to 50 K has been inferred (Vidal-Madjar et al. 1994, Jolly et al. 1996). On the other hand, CO (1–0) observations by Savoldini & Galletta (1994) resulted in an upper limit on the line intensity, $< 0.5\,\mathrm{K\,km\,s}^{-1}$. Savoldini & Galletta interpreted their upper limit in terms of a high depletion of CO, as compared to interstellar gas (a view taken quite often in the literature: e.g. Vidal-Madjar et al. 1994, Lagrange et al. 1995, Dent et al. 1995). However, these results could simply mean that the millimeter observations were suffering from beam dilution effects. These could be reduced by observing at a higher frequency, e.g. that of the (2–1) transition (by a factor of up to four using the same telescope). In addition, at temperatures above 20 K, the $J$=2 level of CO is preferably populated as compared to $J$=1, resulting in a line intrisically at least twice as strong. Consequently, CO (2–1) observations are potentially more sensitive and appear comparatively more powerful to probe any CO gas in the circumstellar disk of $\beta$ Pic. In this paper, we report on such observations. CO (2–1) observations of $\beta$ Pic were already reported by Dent et al. (1995), who interpreted their results in terms of thermodynamic equilibrium (LTE) at a single disk temperature. In the present study we are addressing the molecular excitation and line transfer in the disk in a more quantitative way. In addition to CO, we observed $\beta$ Pic also in the CS (2–1)

*Send offprint requests to*: R. Liseau

$^\star$ Based on observations collected with the Swedish ESO Submillimeter Telescope, SEST, in La Silla, Chile.

line in order to study to what extent the chemistry in the disk might differ from that in interstellar clouds.

Artymowicz (in preparation) has proposed that SiO is an abundant form of Si-bearing gas produced in evaporative collisions between the silicate dust grains. Frequent, energetic grain-grain collisions in the innermost part of the disk ($r < 20$ AU) could produce significant amounts of SiO gas, although this region appears largely dust depleted (Lagage & Pantin 1994; see also below, Fig. 5). Compared to CO, the significantly larger dipole moment of SiO offers the advantage of detecting relatively smaller molecular concentrations from millimeter observations. Taking an observational approach, we selected a vibrationally excited transition of SiO to trace any hot and very dense gas ($v$=2, $J$=2–1) and the low lying ($v$=0, 2–1) line to probe the more probable, cooler component at moderate densities.

First results were presented by Liseau & Artymowicz (1997), which were based on an analytical analysis using average disk quantities. In this paper, we offer a more detailed approach taking the disk structure fully into account. Our earlier findings are entirely confirmed by the more rigorous treatment of this paper.

## 2. Observations

We observed $\beta$ Pic with the Swedish ESO Submillimeter Telescope (SEST) in December $14-19$, 1994. Formally, the equatorial coordinates of $\beta$ Pic we used were $\alpha_{1950.0} = 05^{\rm h}46^{\rm m}05\overset{\rm s}{.}873$ and $\delta_{1950.0} = -51^\circ\ 04'\ 58\overset{''}{.}35$. These coordinates are proper motion corrected to the epoque of our observations. The radial velocity of the star is not very well determined: early works show a spread by a factor of nearly two and Hoffleit & Jaschek (1982) assigned the comment *variable?* to their value of $+20$ km s$^{-1}$ in the Bright Star Catalogue. A more recent discussion is found in Vidal-Madjar et al. (1994), who place the CO absorption features at the heliocentric velocity $v_{\rm hel} = +21 \pm 3$ km s$^{-1}$. This corresponds to $+2.3$ km s$^{-1}$ on the LSR velocity scale, which is commonly exploited in galactic millimeter work.

In the 3 millimeter band, we used a cooled Schottky mixer as frontend, whereas at the CO (2–1) frequency ($\lambda = 1.3$ mm) an SIS receiver was exploited. As backend we used a 2000 channel acousto-optical spectrometer (AOS) with 43 kHz wide channels, thus covering a total bandwidth of 86 MHz. In terms of radial velocity, the resolution at the various spectral line frequencies ranges between 0.1 and 0.3 km s$^{-1}$ ($2\,\Delta v$, see: Table 1). With the exception of the SiO ($v$=0) line, we observed two transitions simultaneously, splitting the AOS into two halves, so that the spectral coverage ranges from about 50 to 300 km s$^{-1}$ (see: Fig. 1).

Depending on the frequency of observation, the beam of the 15 m SEST subtends a sky angle of about one third of an arcminute to one arcmin (Table 1). The mode of observation selected was wide dual beam switching, placing either the star or a reference position about $12'$ away into the telescope beam ($11'37''$ beam throw in positive and negative azimuth respectively). The pointing stability of the telescope was regularly checked by observing the SiO maser source R Dor, only some $10^\circ$ distant from $\beta$ Pic, and was found to be excellent during these observations (within $1\overset{''}{.}2$ rms). The relative alignment of the 1 and 3 millimeter beams is known to be within $3''$.

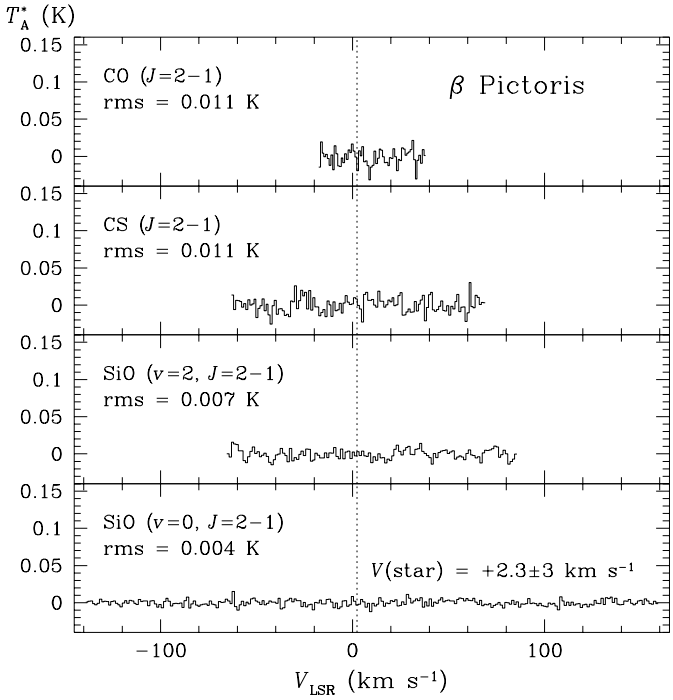


**Fig. 1.** The observed millimeter wave spectra at four molecular line transitions of the $\beta$ Pic system. The stellar (photospheric) radial velocity of $\beta$ Pic is indicated by the vertical dotted line. CO (2–1) (top) was observed simultaneously with either CS or the highly excited SiO transition ($v$=2) by splitting the AOS into two halves. This resulted in less spectral coverage than for the low lying SiO transition ($v$=0, at bottom). The spectral resolution has been degraded somewhat by binning the velocity channels to about 1 km s$^{-1}$ (SiO$_{v=0}$ : 1.2 km s$^{-1}$, SiO$_{v=2}$ : 1.2 km s$^{-1}$, CS : 1.1 km s$^{-1}$, CO : 0.9 km s$^{-1}$). The resulting values of the rms noise are shown in each panel

Calibrations were done internally using a chopper wheel load resulting in the $T_{\rm A}^*$ scale (Ulich & Haas 1976). The atmospheric conditions were generally stable during our run. However, in local summer, the La Silla zenith optical depth at 230 GHz was quite high, about 0.5 (Table 1). From observations of Ori A we deduce that the day to day reproducibility of the signal was within an uncertainty of about 10 – 20%.

## 3. Reductions and results

### *3.1. Continuum radiation at 1.3 and 3.45 mm*

The individual spectrum pairs for either beam throw were added and total averages were formed, where the weighting was done with respect to the rms noise in the spectral scans. The resulting spectrograms testified to the overall stability of the system and of the sky: linear baseline fits resulted in offsets from the zero level by some fraction of a milli-Kelvin (mK). As the average $T_{\rm A}^*$ over the whole spectral band is of this order, it is clear that any continuum emission from the $\beta$ Pic disk would have to be below this level. Specifically, strict upper limits of 8 mJy

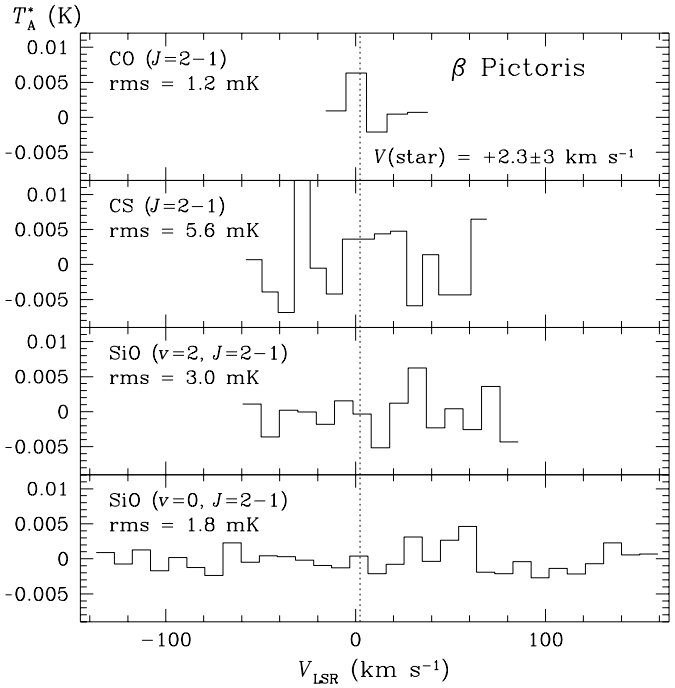


**Fig. 2.** As Fig. 1, but the intensity scale ($T_A^*$) has been expanded by one order of magnitude: the spectra have been rebinned at the characteristic scale of the Keplerian velocity of about 10 km s$^{-1}$ ($SiO_{v=0}$ : 9.5 km s$^{-1}$, $SiO_{v=2}$ : 9.7 km s$^{-1}$, CS : 8.4 km s$^{-1}$, CO : 10.7 km s$^{-1}$)

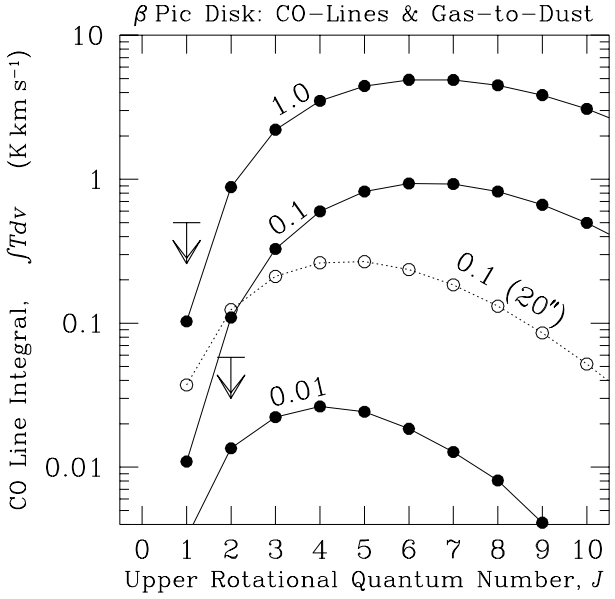


**Fig. 3.** Integrated CO line intensity, $\int T\,dv$, versus upper rotational quantum number, $J$, of the transition for the disk model described in the text. A telescope aperture of 15 m has been assumed for the calculations, depicted by the solid lines. The dashed curve corresponds to a fix beam size instead, viz. HPBW = 20″. The values of the parameter, $m_{gas}/m_{dust}$, are indicated next to each curve. Observational results (in the main beam temperature scale) are indicated by the upper limit symbols, where (1–0) is from Savoldini & Galletta (1994) and (2–1) from the present investigation. For both models and observations, the integrations have been performed ±5 km s$^{-1}$ about the systemic velocity

at 86 GHz (3.45 mm) and of 40 mJy at 230 GHz (1.3 mm) are implied by these measurements. The latter value is in agreement with the bolometer datum obtained with the same telescope by Chini et al. (1991), viz. $S_{1.3\,mm} = 24.9 \pm 2.6$ mJy. From the disk model described in Sect. 4 we find $S_{3.45\,mm} = 1.2$ mJy, which is clearly also in agreement with our observations.

### *3.2. Molecular line emission: CO, CS and SiO*

Our molecular line searches gave similarly negative results: in no case did we directly detect any signal above the limiting noise, $T_{rms}$, given in Table 1, in spite of very deep integrations. In order to enhance the recognizability of presumably very faint signals we also changed the sky frequency towards $\beta$ Pic by ±50 km s$^{-1}$. This procedure was demonstrably warranted as we first found an apparently solid detection of the SiO ($v$=0, 2–1) line after some 17 000 s of on-source integration (sic!). At 1 km s$^{-1}$ resolution, the level of the rms noise is at only 7 mK in this spectrogram. Clearly, this erroneous result was due to some very low-level, about 20 km s$^{-1}$ wide and centred approximately on the stellar radial velocity, irregularities of the receiver response (see: Figs. 2 and 6).

Over the observed bandwidths, this direction of the Galaxy ($\ell^{II}$ = 258.°4, $b^{II}$ = –30.°6) is virtually void of any molecular material within some tens of arcmin surrounding $\beta$ Pic, making $\beta$ Pic an optimum reference position for galactic millimeter line work. The rms levels of the noise temperature, in $T_A^*$, are for SiO ($v$=0, $J$=2–1) 6 mK, for SiO ($v$=2, $J$=2–1) 10 mK, for CS ($J$=2–1) 16 mK and for CO ($J$=2-1) 25 mK per velocity channel, $\Delta v$. Binning the channel data into widths of about 1 km s$^{-1}$, decreases the noise to the values indicated in Fig. 1. Evidently, for the transitions of our primary interest, low-excitation SiO and CO ($J$=2–1), the achieved sensitivity of our measurements is $\delta T/T < 2\,10^{-5}$. In Fig. 2, the data have been binned at the presumed characteristic Keplerian velocity of the $\beta$ Pic disk. For CO (2–1), this can be compared to the 15 m JCMT observations by Dent et al. (1995), who obtained at 12 km s$^{-1}$ binning an upper limit a factor of three times higher ($T_A^* < 4.2$ mK, 1 $\sigma$).

## 4. Discussion

### *4.1. The 'enigmatic' CO source of $\beta$ Pic*

Our CO (2–1) observations with the SEST should be directly comparable to the 1.3 mm continuum observations by Chini et al. (1991), since these were obtained with the same telescope and, hence, with the same beam size. Chini et al. modeled their results in terms of thermal dust emission from the circumstellar disk of $\beta$ Pic. The temperature and density of the dust were described by radial power laws. The size distribution of the grains includes particles as large as 4.3 mm. The lower limit to the *dust* mass of 0.44 $M_\oplus$ within the SEST beam (∼ 400 AU) was derived. According to these authors their derived dust mass is

**Table 1.** Molecular line observations of $\beta$ Pic at the 15 m SEST

| Rest frequency (MHz) | Transition $(J = 2-1)$ | $E/k$ (K) | HPBW ($''$)/(AU)[c] | $\eta_{\rm mb}$ | $\Delta v$ (km s$^{-1}$) | $\overline{T_{\rm sys}}$ [a] (K) | $\overline{\tau_{\rm atm}}$ [a] | $t_{\rm int}$ (hr) | $T_{\rm rms}$ [b] (K) |
|---|---|---|---|---|---|---|---|---|---|
| 85 640.456 | SiO $(v = 2)$ | 3526 | 60/1158 | 0.75 | 0.1512 | 334 | 0.06 | 6.4 | 0.010 |
| 86 846.998 | SiO $(v = 0)$ | 6 | 60/1158 | 0.75 | 0.1491 | 276 | 0.04 | 12.0 | 0.006 |
| 97 980.968 | CS $(v = 0)$ | 7 | 53/1023 | 0.60 | 0.1321 | 449 | 0.05 | 6.0 | 0.016 |
| 230 537.990 | CO $(v = 0)$ | 16 | 23/444 | 0.38 | 0.0562 | 893 | 0.51 | 12.4 | 0.025 |

Notes to the table:
[a] Average values of the total system noise temperature, $T_{\rm sys}$, and of the atmospheric zenith opacity, $\tau_{\rm atm}$, during the observations.
[b] $T_{\rm rms}$ is the rms-fluctuation of the chopper-wheel calibrated antenna temperature, $T_{\rm A}^{*}$, per velocity channel, $\Delta v$, after the on-source integration, $t_{\rm int}$.
[c] Physical size of the half power SEST beam at the distance of 19.3 pc.

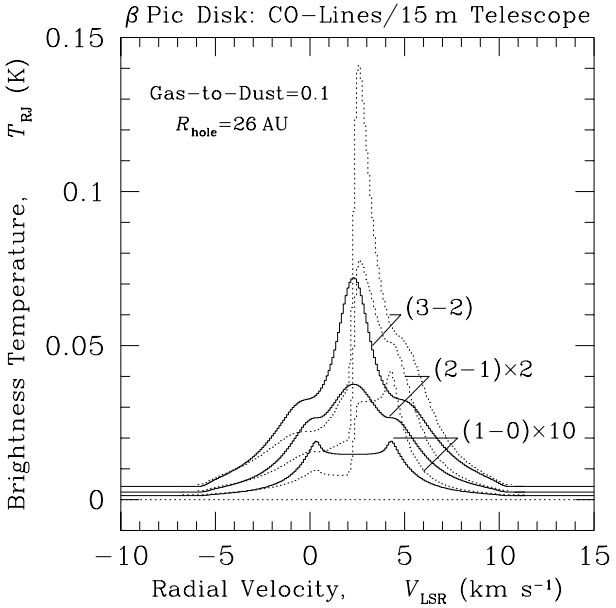


**Fig. 4.** CO line profiles for the $\beta$ Pic disk model described in the text. The numerical resolution is 0.1 km s$^{-1}$ in velocity and 1.25 AU in the spatial coordinates. An inner hole radius of 26 AU and $m_{\rm gas}/m_{\rm dust}$=0.1 have been assumed throughout. The beams of a 15 m telescope are taken as 46$''$ (1–0), 23$''$ (2–1) and 15$''$ (3–2) and the model continuum fluxes are 2.6 mJy (2.6 mm), 25 mJy (1.3 mm) and 83 mJy (0.8 mm), respectively. The curves drawn with solid lines assume axial symmetry for the density distribution. The dotted profiles refer to a non-symmetric disk model (at phase $n\,\pi$), where the power law exponent of the density distribution has been changed by $\pm 15\%$ in the two azimuthal halves of the disk

comparable to the mass of the gas in the disk, i.e. $m_{\rm gas}/m_{\rm dust}$ would be of order unity and much lower than the average interstellar value of about one hundred (Hildebrand 1983).

Adopting the physical structure of the $\beta$ Pic disk from the model by Chini et al., we computed the expected CO $(J \rightarrow J-1)$ emission by varying the gas-to-dust mass ratio, but keeping the CO abundance relative to hydrogen fixed throughout the disk [at the interstellar medium value, $X({\rm CO}) = 8\,10^{-5}$; van Dishoeck et al. 1993 and references therein]. The details of these calculations are presented by Liseau (in preparation), but a basic description of our treatment of the line emission from the disk model is provided in Appendix A. To be directly compatible with the results by Chini et al. we used the pre-Hipparcos distance to the star, viz. 16.4 pc, which will not, however, affect our general conclusions below. The parameters of the $\beta$ Pic disk model are presented in Table 2.

**Table 2.** Adopted parameters for the $\beta$ Pic system

| | | |
|---|---|---|
| Star | | |
| | $d$ (pc) | 16.4 (see: Sect. 4.1) |
| | $v_{\rm hel}$ (km s$^{-1}$) | +21 |
| | $v_{\rm LSR}$ (km s$^{-1}$) | +2.3 |
| | Sp. Type | AV 5 |
| | $T_{\rm eff}$ (K) | 8 200 |
| | $M_\star$ (M$_\odot$) | 1.8 |
| | $R_\star$ (R$_\odot$) | 1.7 |
| Disk | | CO Model/SiO Model |
| | $R_{\rm disk}$ (AU) | 440/1000 |
| | $R_{\rm hole}$ (AU) | 26 (gas and dust)/(dust only) |
| | $n({\rm H_2})(r)$ (cm$^{-3}$) | $9.785\,10^{6}\,(r/26\,{\rm AU})^{-2.5}\,\frac{m_{\rm gas}}{m_{\rm dust}}$ |
| | $T(r)$ (K) | $110\,(r/26\,{\rm AU})^{-0.3}$ |
| | Inclination, $i$ ($^\circ$) | 3 |
| | Flaring, $h(r)/r$ (rad) | 0.03/0.02 |

In Fig. 3, the CO line integral, $\int T_{\rm RJ}\,dv$, as function of the upper rotational level, $J$, is shown together with the observed upper limits, $\int T_{\rm mb}\,dv$, for the (1–0) and (2–1) lines. As expected (Sect. 1), maximum line flux is generally found for transitions from $J \geq 4$, i.e. higher than those hitherto observed from the ground.

Both model profiles and observations have been integrated over $\pm 5$ km s$^{-1}$ about the line center. The presented models have been computed for the gas-to-dust ratios $m_{\rm gas}/m_{\rm dust}$ = 1.0, 0.1 and 0.01. For relatively high values, the gas densities in the disk are sufficiently high to drive the CO lines into LTE, whereas for $m_{\rm gas}/m_{\rm dust}$ = 0.01, the excitation of the molecules is subthermal in most parts of the disk. It

is evident from the figure that the observational results rule out any 'normal' gas-to-dust mass ratio of 100. In particular, $m_{\rm gas}/m_{\rm dust} < 0.1$ ($< 0.05$, $1\,\sigma$) is implied by our measurement ($\int T_{\rm mb}\,dv < 0.058\,{\rm K\,km\,s^{-1}}$, $1\,\sigma$).

In Fig. 4, we present the profiles of low-$J$ CO lines most readily observable from the ground, i.e. (1–0), (2–1) and (3–2). In all cases, an antenna of 15 m aperture has been assumed (e.g. SEST, JCMT). The observed continuum fluxes are reasonably well reproduced by the model [$S_{0.8\,\rm mm} = 83$ mJy (observed: $80 \pm 14$ mJy, Zuckerman & Becklin 1993) and $S_{1.3\,\rm mm} = 25$ mJy (observed: $24.9 \pm 2.6$ mJy, Chini et al. 1991)]. According to this particular disk model, kinetic temperatures are $> 45$ K everywhere and the *average* column density of widespread CO in the gas phase is $N({\rm CO}) < 10^{15}\,{\rm cm^{-2}}$ ($3\,10^{14}\,{\rm cm^{-2}}$ for $m_{\rm gas}/m_{\rm dust} = 0.05$). This strict limit is not particularly sensitive to the choice of parameter values. For instance, in the figure, the dashed profiles refer to a change by $\pm 15\%$ about the nominal value of the power law exponent of the density distribution (Table 2) in the two azimuthal halves of the disk, yielding still about the same $N({\rm CO})$. However, the line profiles would, of course, change quite dramatically (and with time), as is exemplified in the figure. In principle, such non-axisymmetric matter distribution, if present (e.g. Kalas & Jewitt 1995), could thus be used to infer the sense (and rate) of rotation of the disk, which could be compared with the rotation of the host star (see the Solar System).

The high gas temperatures and the upper limit on the CO column density implied by this disk model, which fits the dust continuum observations, are *both* difficult to reconcile with the CO absorption features in the UV (Vidal-Madjar et al. 1994, Jolly et al. 1996). The UV-CO feature, which is at the systemic (stellar) radial velocity, has been persistent over the years since its discovery with the IUE and model fits to the observed profiles indicate the absorbing CO gas to be at very low temperatures. This gas should be, therefore, far away from the star and resides presumably in the outer regions of the disk ($\gg 100$ AU). In addition, the UV models imply a relatively healthy column density of CO molecules [$N({\rm CO}) > 10^{15}\,{\rm cm^{-2}}$]. The apparent absence of molecular features at long wavelengths has commonly been explained in terms of photo-dissociation of the molecules (e.g. Dent et al. 1995). There are at least two difficulties with this explanation. First, dissociation should affect the 'UV-CO' as much as the 'mm-CO' – to the molecules, human observing mode should make little difference. Secondly, recent detailed model calculations made by Rentzsch-Holm et al. (1998) indicate that the stellar (and interstellar) UV field might not be sufficiently strong to largely dissociate the CO molecules in the $\beta$ Pic disk.

A more obvious solution to this enigma seems to be, then, that the CO gas is not widespread throughout the disk (as assumed in our model), but is confined to a relatively distant, localized region (cloud/ring etc.) in front of the star. Such CO 'cloudlet' would be easily seen in absorption against the stellar continuum, but its emission impossible to be detected by our mm-wave observations because of heavy beam dilution.

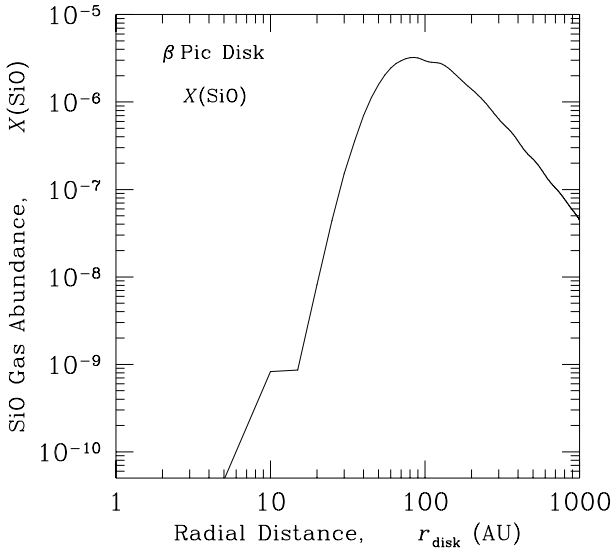


**Fig. 5.** Radial distribution of the SiO gas abundance according to the collisional production model discussed in the text. The hydrogen density distribution follows the disk model by Chini et al. (1991) for $m_{\rm gas}/m_{\rm dust} = 0.1$

### *4.2. An upper limit to the hydrogen mass of the $\beta$ Pic disk*

For the assumed standard value of $X({\rm CO})$, the upper limit to the CO column density derived in the previous section implies an upper limit to the average column density of hydrogen through the disk, $N({\rm H}) < 10^{19}\,{\rm cm^{-2}}$ ($N({\rm H_2}) < 4\,10^{18}\,{\rm cm^{-2}}$). This is of the same order as the value derived from optical/UV and radio work. From an LTE analysis of *metal* lines seen toward $\beta$ Pic, Lagrange et al. (1995) estimated the hydrogen column at (1–2) $10^{19}\,{\rm cm^{-2}}$, assuming solar abundances. Based on HI 21 cm observations, also Freudling et al. (1995) arrived at an upper limit to the hydrogen column density of that order. In conclusion, there seems to be no need to invoke a CO-to-$H_2$ ratio in the $\beta$ Pic disk, which is very much different from the canonical interstellar medium value. In other words, we do not find any convincing evidence that gaseous CO should be significantly (by orders of magnitude) depleted in the disk.

Based on the dust mass obtained by Chini et al. (1991), our CO (2–1) result implies then that the gas mass of the $\beta$ Pic disk (within 440 AU) is not likely to exceed a few hundredths of an Earth mass ($< 0.02\,{\rm M_\oplus}$). We conclude, therefore, that these results are suggestive of the fact that the $\beta$ Pic disk is largely devoid of primordial gaseous material such as hydrogen and carbon monoxide. This conclusion supports the idea that the early nebula around $\beta$ Pic indeed disappeared long ago, i.e. it has been consumed during planet formation and/or was blown out in an early, intense mass loss episode. Such scenario is heuristically purported by the CO detections of Vega-like systems by Zuckerman et al. (1995), all of which are considerably younger than $\beta$ Pic, whose age is estimated at $\gtrsim 80$ Myr (Crifo et al. 1997).

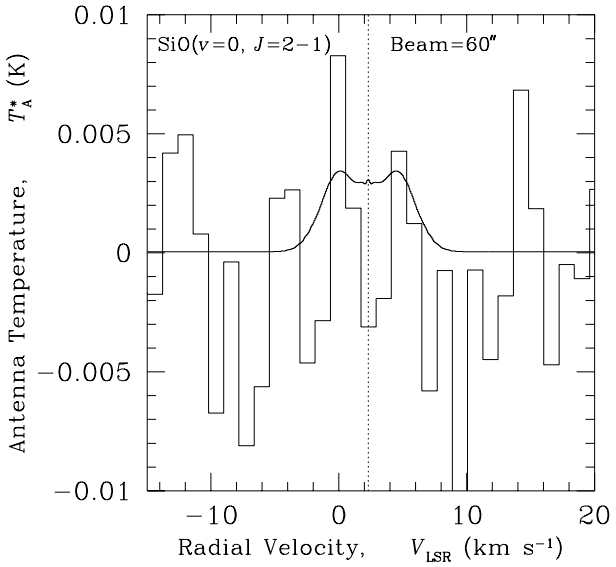


**Fig. 6.** The predicted line profile for SiO (2–1), ($v$=0), (in the $T_A^*$ scale) observed with a 15 m telescope (60″ beam) is shown by the solid line. The at 1 km s$^{-1}$ rebinned SEST data are displayed as histogram

### *4.3. Presently produced SiO gas in the $\beta$ Pic disk*

Artymowicz (in preparation) considers the possibility of the abundant presence of disk gas other than hydrogen or carbon monoxide, viz. silicon bearing molecular gas in particular. This gas is thought to be mainly produced during collision processes of the silicate grains, which constitute most of the mass of the particulate disk. Modeled gas production rates maintain, in the steady state, SiO masses of the order of $M(\mathrm{SiO}) \leq 10^{22}$ g. The disk model considered in the present context differs from the previous one (e.g., the disk extends to 1000 AU) and its parameters are listed in Table 2.

For the hydrogen gas in the disk we adopt the Chini et al. model for $m_{\rm gas}/m_{\rm dust} = 0.1$, which is considered an upper limit and when combined with the Artymowicz model results in the radial distribution of the SiO abundance, $X(\mathrm{SiO})$, shown in Fig. 5. From the figure it is evident that for the bulk of the $\beta$ Pic disk, SiO abundances are supposedly very much larger than what is normally found in the interstellar medium (van Dishoeck et al. 1993 and references therein). Proceeding as before for CO, we computed the expected SiO line emission within the beam of our observation, the result of which is presented in Fig. 6 (numerical resolution in velocity is 0.075 km s$^{-1}$ and in the spatial coordinates 5 AU). For $r < 40$ AU, densities are higher than the critical density of the transition ($\sim 4\,10^5$ cm$^{-3}$), thermalizing the level populations, whereas in the outer parts of the disk the excitation becomes subthermal. The average SiO column density through the disk is $N(\mathrm{SiO}) < 1.5\,10^{12}$ cm$^{-2}$ and the emission is optically thin from most parts of the disk.

Although the rms level in our SEST observation of $\beta$ Pic in SiO (2–1) is very low, the predicted line would still be buried in the noise (see: Fig. 6). As such, these observations are neither in conflict with nor are they able to confirm the predictions of the SiO production model. The test of this model would require observations at significantly higher angular resolution. By matching the telescope beam to the size of $\max X(\mathrm{SiO})$ (see: Fig. 5), viz. to $\sim 5''$, a much higher beam filling could be achieved. This would, as such, require an operating mm-interferometer. For a 5″ beam, the SiO disk model predicts a peak line brightness temperature of nearly 5 K, which appears quite feasible for future testing.

## 5. Conclusions

Our main conclusions from this work can be summarized as follows:

- Sensitive CO (2–1) observations of $\beta$ Pic with the SEST provided merely an upper limit on the line. We combine these observations with the dust continuum result by Chini et al. (1991), obtained at the same wavelength and with the same telescope, in a model of the $\beta$ Pic disk. Comparing predicted CO line intensities with the observed upper limits leads to an upper limit on the gas-to-dust mass ratio in the disk of $m_{\rm gas}/m_{\rm dust} < 0.1$. This implies that at most a few $10^{-2}$ M$_\oplus$ of hydrogen gas reside at present in the circumstellar disk of $\beta$ Pic.
- The derived limiting CO column density ($<10^{15}$ cm$^{-2}$) refers to regions in the disk, where temperatures are significantly higher than those inferred by Vidal-Madjar et al. (1994) and by Jolly et al. (1996) from UV absorption features in the stellar spectrum and which correspond to a CO column $>10^{15}$ cm$^{-2}$. It seems likely, therefore, that this gas is not widespread throughout the disk but confined to a localized region. An additional conclusion is that the available observational evidence does not require any severe CO under-abundance with respect to hydrogen.
- Very sensitive SEST observations of $\beta$ Pic in the SiO ($v$=0, $J$=2–1) line did not detect the postulated source. We find it most likely that insufficient filling of the 60″ telescope beam is responsible for this failure. The testing of the theory of SiO gas production from grain-grain collisions in the disk and, eventually, the mapping of the rotation curve of the $\beta$ Pic disk will have to await the next generation of millimeter wave interferometers in the southern hemisphere.

*Acknowledgements.* We wish to thank the SEST staff for their skillful and enthusiastic support during the observations. This research has been supported by the Swedish Natural Science Research Council (NFR) and benefited from a grant by the *Anna-Greta och Holger Crafoord* Foundation.

## Appendix A: spectral line emission from a circumstellar disk

We consider a simple model of an inclined, slightly flared disk in Keplerian rotation. Using Cartesian coordinates, and with the $y$-axis in the plane of the sky, the disk midplane ($xy$-plane) is inclined with respect to the line of sight by an angle $i$. The disk is rotating about the $z$-axis, along the azimuthal angle $\phi$. The vertical flaring of the disk, $h(r)/r$, is considered a constant.

The physical variables are assumed not to change significantly in the $z$-direction, but to have only radial dependencies, where the radial distance from the star is $r = \sqrt{x^2+y^2}$ and $r \geq R_{\rm star}$, the stellar radius. The component of the velocity along the observer's line of sight (the 'radial' velocity field) is then given by

$$v_{\rm rad}(r) = \left(\frac{G\,M_{\rm star}}{r}\right)^{\frac{1}{2}} \cos i \sin\phi, \tag{A1}$$

where $G$ is the gravitational constant and $M_{\rm star}$ is the mass of the central star. Eq. (A1) describes a set of iso-velocity surfaces (e.g. Gómez & D'Alessio 1995) and, by virtue of the Doppler effect, determines the frequency scale of the spectral line emission, the emergent intensity of which is found from

$$I_\nu(x,y) = B_\nu(T_{\rm bg})\, e^{-\tau_\nu} + B_\nu(T_{\rm ex})\left(1-e^{-\tau_\nu}\right), \tag{A2}$$

where $B_\nu(T)$ is the Planck function. Background radiation fields are specified through $T_{\rm bg}$, whereas the intrinsic disk field is determined by the excitation temperature, $T_{\rm ex}$. Thus, $B_\nu(T_{\rm ex})$ is the line source function, $S_{\nu,\,\rm line}$. Hence, with obvious notations

$$S_{\nu,\,\rm line}(x,y) = B_\nu(T_{\rm ex}) = \frac{2\,h\,\nu^3}{c^2}\left[\frac{g_u}{g_l}\frac{n_l}{n_u} - 1\right]^{-1}. \tag{A3}$$

$T_{\rm ex}$ is obtained from the solution of the rate equations for statistical equilibrium of radiative and collisional excitations, i.e. from the (fractional) energy level populations, $f_u = n_u/n_{\rm tot}$, where $n_{\rm tot}$ corresponds to the number of energy levels considered. The level populations are found by inverting the matrix equation for the transition probabilities, $P_{ij}$ (e.g., Spitzer 1978). Hence, in the steady state,

$$\frac{d}{d\,t}\,\boldsymbol{n} = \boldsymbol{0} = \boldsymbol{P}\,\boldsymbol{n}, \tag{A4}$$

where $\boldsymbol{P}$ is a matrix of dimension $n_{\rm tot} \times n_{\rm tot}$ and $\boldsymbol{n}$ is a vector containing $n_{\rm tot}$ elements. In our models, $n_{\rm tot}$= 50 for CO with Einstein $A$-values from Chackerian & Tipping (1983) and collision rate constants from Green & Thaddeus (1976) and Green & Chapman (1978). For SiO, $n_{\rm tot}$= 21 with molecular data from Tipping & Chackerian (1981) and Turner et al. (1992).

To obtain the line intensity to be received by the observer, the source brightness distribution is convolved, at each frequency, with the diffraction pattern of the telescope (the 'beam'). For simplicitity, the beam is here represented by a circular Gaussian with the full width at half power $b$. Hence, at any relative position $(x',y')$ in the sky

$$I_{\nu,\,\rm obs}(x',y') = \frac{4\,\ln 2}{\pi\,b^2}$$
$$\iint I_\nu(x,y)\,\exp\left[-4\,\ln 2\frac{(x-x')^2+(y-y')^2}{b^2}\right] dy\,dx\sin i. \tag{A5}$$

The optical depth at frequency $\nu$ is obtained as the sum of (molecular) line and (dust) continuum optical depth, i.e. $\tau_\nu = \tau_{\nu,\,\rm line} + \tau_{\nu,\,\rm dust}$. The line optical depth is given by

$$\tau_{\nu,\,\rm line}(v) = \left(\frac{c}{2\,\pi^{\frac{1}{2}}\,\nu}\right)^3 \frac{A_{ul}}{v_{\rm th}}\left[\exp\left(\frac{h\,\nu}{k\,T_{\rm ex}}\right) - 1\right]$$
$$f_u\,X_{\rm mol}\,N({\rm H}_2)\,\exp\left[-\frac{(v-v_0)^2}{v_{\rm th}^2}\right], \tag{A6}$$

where the column density of hydrogen

$$N({\rm H}_2) = \frac{\iiint n({\rm H}_2)\,dx\,dy\,dz}{\iint dy\,dx\sin i} \sim h(r)\,n({\rm H}_2)\csc i. \tag{A7}$$

$A_{ul}$ is the Einstein transition probability and $X_{\rm mol}$ is the molecular abundance with respect to hydrogen, $H_2$. $v_0$ is the line center velocity (systemic radial velocity) and the broadening is assumed purely thermal at the local (dust) temperature, i.e. $v_{\rm th}(x,y) = \sqrt{2\,k\,T/(A_{\rm mol}\,{\rm amu})}$, where $A_{\rm mol}$ is the molecular mass number.

The continuum optical depth is assumed constant over the line and computed as

$$\tau_{\nu,\,\rm dust} = \kappa_0\left(\frac{\lambda_0}{c}\,\nu\right)^\beta \mu\,m_{\rm H}\,N({\rm H}_2)\,\Big/\,\frac{m_{\rm gas}}{m_{\rm dust}}, \tag{A8}$$

where $\mu$ is the mean molecular weight of the gas, assumed molecular ($\mu = 2.4$). For the $\beta$ Pic disk, we adopt the density and temperature distributions of the dust of Chini et al. 1991, which are expressed as radial power laws. To obtain the distribution of the molecular hydrogen gas, $n(H_2)$, the dust density law has been scaled by the (constant) gas-to-dust mass ratio. For computational convenience, the frequency dependence of the *dust* opacity is expressed in power law form (Hildebrand 1983), with the parameters $\kappa_0 = \kappa_\nu(\lambda_0)$ and $\beta$ adjusted such that the disk model of the dust emission fits the mm/submm observations by Chini et al. (1991) and by Zuckerman & Becklin (1993), i.e. $\kappa_0 = 4\,{\rm cm}^2\,{\rm g}^{-1}$ at $\lambda_0 = 250\,\mu$m with $\beta = 1.5$.

We have computed an analogue of and compared with the model results for HL Tau obtained by Gómez & D'Alessio (1995) and our line to continuum ratios are in very good agreement with what can be estimated from the profiles in their Fig. 3. We also found very good agreement with Yamashita et al. (1993) regarding the profile shape of the CO (1-0) line for $\varepsilon$ Eri [however, our result for the integrated line intensity (in the $T_{\rm A}^*$ scale) for their model is a factor of about 4 below that given in their Table 2].

## References


Artymowicz P., 1997, Ann. Rev. Earth Planet Sci. 25, 175

Backman D.E., Paresce F., 1993, in: Levy E.H., Lunine J.I. (eds.) Protostars and Planets III, Tuscon: Univ. Arizona Press, p. 1253

Beust H., Vidal-Madjar A., Ferlet R., Lagrange-Henri, 1994, Ap&SS 212, 147

Chackerian Jr. C., Tipping R.H., 1983, J Mol Spec 99, 431

Chini R., Krügel E., Shustov B., Tutukov A., Kreysa E., 1991, A&A 252, 220
Crifo F., Vidal-Madjar A., Lallement R., Ferlet R., Gerbaldi M., 1997, A&A 320, L 29
Dent W.R.F., Greaves J.S., Mannings V., Coulson I.M., Walther D.M., 1995, MNRAS 277, L 25
Freudling W., Lagrange A.M., Vidal-Madjar A., Ferlet R., Forveille T., 1995, A&A 301, 231
Gómez J.F., D'Alessio P., 1995, Rev Mex AA (Ser. Conf.) 1, 339
Green S., Chapman, 1978, ApJS 37, 169
Green S., Thaddeus P., 1976, ApJ 205, 766
Habing H.J., Bouchet P., Dominik C., et al., 1996, A&A 315, L 233
Hildebrand R.H., 1983, QJRAS 24, 267
Hoffleit D., Jaschek C., 1982, The Bright Star Catalogue, Yale University Observatory
Jolly A., Lagrange A.M., Mc Phate J., et al., 1996, in: Jansen D.J., Hogerheijde M.R., van Dishoeck E.F. (eds.), Molecules in Astrophysics, Probes & Processes, IAU Symp. 178, Abstract Book, p. 263
Kalas P., Jewitt D., 1995, AJ 110, 794
Lagage P.O., Pantin E., 1994, Nature 369, 628
Lagrange A.M., 1995, Ap&SS 223, 19
Lagrange A.M., Vidal-Madjar A., Deleuil M., et al., 1995, A&A 296, 499
Liseau R., Artymowicz P., 1997, in: Eiroa C., Alberdi A., Thronson H., de Graauw T., Schalinski C.J. (eds.), Infrared Interferometry: Astrophysics & the Study of Earth-like Planets, Kluwer Acad. Publ., p. 55
Renztsch-Holm I., Holweger H., Bertoldi F., 1998, in: Yun J.L. & Liseau R. (eds.) Star Formation with the Infrared Space Observatory, ASP Conf. Ser. 132, p. 275
Savoldini M., Galletta G., 1994, A&A 285, 467
Spitzer L.Jr., 1978, Physical Processes in the Interstellar Medium, John Wiley & Sons, New York
Tipping R.H., Chackerian Jr. C., 1981, J Mol Spec 88, 352
Turner B.E., Chan K.-W., Green S., Lubowich D.A., 1992, ApJ 399, 114
Ulich B.L., Haas R.W., 1976, ApJS 30, 247
van Dishoeck E.F., Blake G.A., Draine B.T., Lunine J.I., 1993, in: Levy E.H., Lunine J.I. (eds.) Protostars and Planets III, Tuscon: Univ. Arizona Press, p. 163
Vidal-Madjar A., Lagrange-Henri A.-M., Feldman P.D., et al., 1994, A&A 290, 245
Yamashita T., Handa T., Omodaka T., et al., 1993, ApJ 402, L 65
Zuckerman B., Becklin E.E., 1993, ApJ 414, 793
Zuckerman B., Forveille T., Kastner J.H., 1995, Nature 373, 494